

Manuscript BJ2003/1507, revised

**Crystal Structure of a Platelet Agglutinating Factor Isolated from the
Venom of Taiwan Habu (*Trimeresurus mucrosquamatus*)**

Running title: Structure of Mucrocetin, a GPIIb Agonist

Kai-Fa Huang^{1,2}, Tzu-Ping Ko¹, Chin-Chun Hung¹, John Chu¹,
Andrew H.-J. Wang^{1,2*} and Shyh-Horng Chiou^{1,2*}

¹Institute of Biological Chemistry, Academia Sinica, Taipei 115, Taiwan

²Institute of Biochemical Sciences, National Taiwan University, Taipei 106, Taiwan

*Corresponding authors:

Dr. Andrew H.-J. Wang, Institute of Biological Chemistry, Academia Sinica, Nankang, Taipei 11529,
Taiwan Tel: 8862-2788-1981 Fax: 8862-2788-2043 E-mail: ahjwang@gate.sinica.edu.tw

and

Dr. Shyh-Horng Chiou, Institute of Biochemical Sciences, National Taiwan University, PO Box 23-106,
Taipei, Taiwan Tel: 8862-2363-9081 Fax: 8862-2363-5038 E-mail: shchiou@gate.sinica.edu.tw

The nucleotide sequences for the mucrocetin α and β -subunits have been deposited in the GenBank database under the accession numbers of AY390533 and AY390534, respectively.

Abbreviations used: GPIIb, glycoprotein IIb; GPIIb-BP, GPIIb-binding protein; vWf, von Willebrand factor; PRP, platelet-rich plasma; CRD, carbohydrate-recognition domain; FL-A, flavocetin-A.

SYNOPSIS

Platelet glycoprotein Ib-binding proteins (GPIb-BPs) from snake venoms are usually C-type lectins, which target on specific sites of GPIb α and elicit distinct effects on platelets. Here, we report a tetrameric platelet-agglutinating factor ($M_r = 121.1$ kDa), termed mucrocetin, purified from the venom of Taiwan habu (*Trimeresurus mucrosquamatus*). Mucrocetin is a GPIb agonist with a distinct binding site from that of flavocetin-A (a snake venom GPIb α antagonist) on GPIb α in spite of the high sequence identity (94.6%) between the two venom lectins. The crystal structure of mucrocetin was solved and refined to 2.8 Å resolution, which shows an interesting crystal packing of six-layer cylinders of doughnut-shaped molecules. The four $\alpha\beta$ -heterodimers are arranged in an unusual square-shaped ring stabilized by four inter-dimer “head-to-tail” disulfide bridges. Detailed structural comparison between mucrocetin and flavocetin-A suggests that their disparate platelet effects are likely attributable to different charge distributions on the putative concave binding surface. A unique positively-charged patch on the binding surface of mucrocetin, formed by Lys¹⁰², Lys¹⁰⁸, Lys¹⁰⁹ and Arg¹²³ in α -subunit coupled with Lys²², Lys¹⁰², Lys¹¹⁶ and Arg¹¹⁷ in β -subunit, appears to be the primary determinant of its platelet-agglutinating activity. Conceivably, this interesting venom factor may provide a useful tool to study platelet agglutination by binding to the GP Ib-IX-V complex.

Key words: snake venom, *Trimeresurus mucrosquamatus*, lectin-like protein, platelet glycoprotein Ib, mucrocetin, flavocetin-A.

INTRODUCTION

The interaction of von Willebrand factor (vWf) A1 domain with the platelet glycoprotein Ib α (GPIb α) is important in mediating the initial tethering and rolling of platelets on the subendothelium of injured vessel walls [1,2]. Several exogenous modulators, such as ristocetin and some venom proteins [3-5], were shown to promote the formation of vWf-GPIb α complex through the binding to the A1 (or A3) domain of vWf. In addition, a number of GPIb α -binding proteins (GPIb-BPs) were found in the venoms of many crotalid and viperid snakes [6,7], which either play the role of GPIb antagonist to block the binding of vWf to GPIb α or behave as the GPIb agonists to induce platelet aggregation or agglutination.

Up to now, several venom GPIb α antagonists and their full-length sequences have been reported (summarized in Table 1) [8-13]. These venom proteins, with the exception of flavocetin-A, exist as $\alpha\beta$ heterodimer of ~27 kDa with the two subunits being ~14 and ~15 kDa. In contrast, flavocetin-A is a tetrameric form of $\alpha\beta$ heterodimers linked by four inter-dimer cystine bridges [14]. These venom factors block ristocetin- or botrocetin-induced aggregation of platelet-rich plasma (PRP), but they had no effect on ADP-induced aggregation. On the other hand, alboaggregin A and B and agglucetin are venom GPIb α agonists (Table 1), capable of directly inducing aggregation or agglutination of washed or fixed human platelets [15,16]. Alboaggregin A and agglucetin were reported to exist in high molecular-mass forms of ~50 kDa, composed of disulfide-linked α , β , γ and δ (or α_1 , α_2 , β_1 and β_2 in agglucetin) subunits, while alboaggregin B is an $\alpha\beta$ heterodimer. The tetrameric alboaggregin A is stronger in terms of inducing platelet aggregation and subsequent release reaction than alboaggregin B [15]. Although these GPIb-BPs are structurally similar and target on the same platelet receptor, they appeared to bind to distinct or partially overlapping sites on GPIb α [10].

Crystal structures of the homologous lectin-like venom proteins showed that the α and β subunits are dimerized by domain swapping, creating a central concave surface which could be important as a binding site for the target molecules [14,17]. The projected loop and the adjoining subunit complete the C-type carbohydrate-recognition domain (CRD) fold. However, they generate a large conformational change on the hinge region classically involved in Ca^{2+} and carbohydrate binding, resulting in the disruption of lectin active site and the loss of carbohydrate-recognizing activity. The work of Mizuno *et al.* on the elucidation of the complex structure between X-bp and the γ -carboxyglutamic acid (Gla) domain of factor X demonstrated that the concave surface is indeed the binding site for the Gla domain [18]. Close structural comparisons suggested that the determinants of lectin-like venom proteins for target recognition may reside on this concave surface which has different surface charge potentials among various venom proteins [19].

In this paper, the crystal structure and biological activity of a platelet-agglutinating factor, mucrocetin, purified from the venom of Taiwan habu (*Trimeresurus mucrosquamatus*) are reported. We found that mucrocetin shows a highly similar 3D structure and a high sequence identity to that of flavocetin-A. Surprisingly, further analysis of platelet-agglutinating activity suggested that mucrocetin is a GPIIb/IIIa agonist with a distinct binding site from that of flavocetin-A on GPIIb/IIIa. Since the binding sites of lectin-like venom proteins on GPIIb/IIIa are not congruent, mucrocetin may offer an elegant case in probing the structural basis of snake venom GPIIb-BPs for the binding and activation of GPIIb/IIIa.

MATERIALS AND METHODS

Reagents

The crude venoms of *T. mucrosquamatus* were obtained from a local snake farm, and the venom glands were kindly provided by the National Institute of Preventive Medicine, Taipei, Taiwan. Lyophilized venom powder of *T. flavoviridis* was purchased from Sigma Chemical. Co. (St. Louis, MO). TSK DEAE-650 anion-exchange resin was obtained from Merck KGaA (Darmstadt, Germany). Sephadex G-100 and Q Sepharose resins, the QuickPrep mRNA preparation kit, and the cDNA Synthesis System Plus Kit were obtained from Amersham Pharmacia (Uppsala, Sweden). Monoclonal antibody CD42b Ab-1 (raised against the platelet GPIb) was purchased from Lab Vision Co. (Fremont, CA). Ristocetin was obtained from Chrono-Log Co. (Havertown, PA). All the other reagents were purchased from either Sigma or Merck.

Isolation and purification of mucroctin and flavocetin-A

Venom components were separated by anion-exchange chromatography on an open column (2.5 × 46 cm) packed with TSK DEAE-650 (M) gel suspension. Approximately 350 mg venom powder was dissolved in 8 ml starting buffer (0.025 M ammonium bicarbonate, pH 7.7) and applied to the column equilibrated with the same buffer. The column was extensively washed by starting buffer and then eluted in a linear gradient of 0.025-0.5 M ammonium bicarbonate, followed by 0.5-1.0 M ammonium bicarbonate, pH 8.0, similar to those described previously [20]. A gel-filtration chromatographic step was carried out on a Sephadex G-100 (S) (1.6 × 120 cm) column, using 0.025 M ammonium bicarbonate at pH 7.8 as the elution buffer. Finally, a HPLC gel-filtration column (Bio-Sil SEC 250-5, 7.8 × 300 mm, Bio-Rad) on a Hitachi liquid chromatograph equipped with a model L-6200 pump and a tunable UV detector was used to further purify the fractions isolated from the above

chromatographic steps.

We also purified flavocetin-A (FL-A) according to the method reported by Taniuchi *et al.* with some modifications [21]. The purified proteins of FL-A were confirmed by platelet assays, N-terminal sequencing and immunoblotting analysis.

Platelet-agglutination assay

Human peripheral blood collected from a healthy volunteer was anticoagulated with 0.1 volume of sodium citrate (3.8%, w/v). In order to prepare human platelet-rich plasma (PRP), the whole blood was centrifuged at $150 \times g$ for 12 min at room temperature. Washed platelet suspension was prepared mainly according to the protocol described previously [22]. Isolated platelets were suspended in Tyrode's solution (0.1% glucose, 0.8% sodium chloride, 0.1% sodium bicarbonate, 0.02% potassium chloride, 0.005% sodium dihydrogen phosphate, 0.02% calcium chloride, and 0.01% magnesium chloride, pH 7.4) and the platelet count was adjusted to $3 \sim 5 \times 10^8$ platelets/ml. Platelet agglutination was performed using an aggregometer (Chrono-Log) at 37°C with stirring (1,000 rpm). The extent of platelet agglutination was continuously monitored for 10 min by turbidmetry and expressed as an increase in light transmission.

Reduction, pyridylethylation and N-terminal sequence analysis of mucrocetin

Mucrocetin (~ 2 nmol) was incubated in 100 μ l of 0.25 M Tris-HCl, pH 8.5 containing 6 M guanidine hydrochloride, 1 mM EDTA and 5% (v/v) β -mercaptoethanol for 16 hr at room temperature. Subsequently, 5 μ l of 4-vinylpyridine was added and the incubation was continued for additional 90 min. After acidification with pure formic acid, S-pyridylethylated subunits were separated and purified by RP-HPLC using a Vydac Protein C4 column (1 \times 25 cm). The eluted

mucrocetin subunits were lyophilized and dissolved in 0.1% (v/v) trifluoroacetic acid, followed by subjecting to N-terminal sequence analysis.

Cloning of mucrocetin cDNA

To prepare the cDNA mixture for PCR cloning, two deep-frozen venom glands from an individual snake were homogenized and poly(A)⁺ RNAs were purified using the QuickPrep mRNA preparation kit. Double-stranded cDNA synthesis was carried out using the cDNA Synthesis System Plus Kit. For the cloning of mucrocetin cDNA, two oligonucleotide primers of sense and antisense orientations based on the highly conserved 5'- and 3'- noncoding regions of cDNAs coding for agkicetin-C [9] and mamushigin [12] with the forward sequence 5'-CTCTGCAGGGAAGGAAGGAA GACCATG-3' and the reverse one 5'-TTGCTTCTCCAGACTTCAC(A/T)CAG C(C/T)G-3' were synthesized. The reactions were subjected to 35 cycles of heat denaturation at 94°C for 1.5 min, annealing the primers to the DNAs at 50°C for 2 min, and DNA chain extension at 72°C for 2.5 min, followed by a final extension at 72°C for 10 min. The PCR products were subcloned into pGEM-T vector, and then transformed into *E. coli* strain JM109. Plasmids purified from positive clones were prepared for nucleotide sequence analysis by automatic fluorescence-based sequencing using a model 373A DNA Sequencing System (Applied Biosystem).

Crystallization and data collection

Purified mucrocetin was concentrated to 52.3 mg/ml by using an ultra-filtration membrane YM-30 (Millipore Amicon, Billerica, MA). The screening for the crystals of mucrocetin was achieved using crystallization screening kits from Hampton Research (Laguna Niguel, CA). Finally, mucrocetin in 0.025 M ammonium bicarbonate at pH 7.8 was mixed with an equal volume of the reservoir (2.5 M 1,6-hexanediol, 0.1 M sodium citrate at pH 5.6) and then crystallized at room

temperature using the hanging-drop vapour-diffusion method. Crystals with their dimensions reaching $0.2 \times 0.15 \times 0.1$ mm appeared within one week. X-ray diffraction data were first collected at Academia Sinica (Taipei, Taiwan) using MSC MicroMax-002 equipped with an R-Axis IV⁺⁺ image-plate detector. Later, data were collected using beam line 41XU at SPring-8 (Hyogo, Japan) with a charge-coupled device (CCD) detector. Finally, more data were collected from beam line 17B2 at NSRRC (Hsinchu, Taiwan) using the similar image-plate detector as above. Data were processed using the HKL package installed on Silicon Graphics Inc. (SGI) O2 workstations [23].

Structure determination and refinement

For molecular replacement search, a 4.5 Å resolution data set collected using an in-house X-ray source and a tetrameric FL-A model generated from the PDB entry 1C3A were employed. By the comparison of space group and unit cell dimension with those of FL-A, the mucrocetin crystal was estimated to contain 3 heterodimers in an asymmetric unit. By using the program CNS [24], 3 rotation function solutions were obtained, as expected, which corresponded to rotations of 62, 78 and 93 degrees about the 4-fold axis. Translation function search based on the 3 rotation function solutions also yielded 3 solutions, with the centers of tetramers remaining aligned with the c-axis and placed at 74.3 Å, 45.9 Å and 14.2 Å from the origin.

Preliminary refinement using the FL-A model while including strict non-crystallographic symmetry (NCS) constraints gave R and R_{free} of 0.278 and 0.335, respectively, using the 3.3 Å data set collected at Spring-8. The resulting Fourier maps showed corresponding densities for most of the different amino-acid residues between FL-A and mucrocetin. Density modification with solvent flipping and 3-fold NCS averaging increased the overall figure of merit from 0.78 to 0.86, but the quality of the map was not significantly improved. Substitution of all amino-acid residues for

the correct sequence of mucrocetin yielded R and R_{free} of 0.282 and 0.312, respectively, after strict-NCS refinement. Subsequent cycles of refinement included manual adjustments of the protein model and addition of water molecules. Finally, further refinement by employing NCS restraints and using the synchrotron data from NSRRC was carried out. The final model of mucrocetin contains 601 water molecules located according to density level of 1.2σ in the $2F_o - F_c$ maps. The atomic coordinates of the mucrocetin structure have been deposited at Research Collaboratory for Structural Bioinformatics (RCSB) Protein Data Bank (accession number: XXXX).

RESULTS

Isolation and purification of mucrocetin and flavocetin-A

Trimeresurus mucrosquamatus venoms were separated by TSK DEAE-650 anion-exchanger column into at least twelve peaks (Figure 1), showing an elution pattern superior to that reported previously [20]. The fractions with strong platelet-agglutinating activity were collected. As judged by SDS-PAGE, a number of proteins in the pooled fraction showed molecular masses larger than 100 kDa under non-reducing condition and distinct from the rest. Therefore, further purification by Sephadex G-100 was carried out, which was followed by a final step of purification using HPLC gel-permeation column to obtain pure mucrocetin. On SDS-PAGE, mucrocetin migrated as two distinct bands of 16 and 14 kDa under reducing condition, and a major band with an apparent molecular mass of 135 kDa under non-reducing condition (Figure 1, *inset*, lanes 2 and 4).

On the other hand, after purification, flavocetin-A (FL-A) was analyzed for the first five amino-acid residues of the two subunits. They are DFDXI and GFXXP (X denoting unidentified residue), in agreement with the α - and β -chain of FL-A, respectively [14]. The purified FL-A was also verified by their strong inhibitory

activity on ristocetin-induced platelet aggregation in human platelet-rich plasma (PRP) (Figure 2D). On SDS-PAGE, mucrocetin shows a similar mass to FL-A under non-reducing condition (Figure 1, *inset*, lanes 3 and 4), while the α -subunit of mucrocetin is slightly larger than that of FL-A under reducing condition (compare lanes 1 and 2). Rabbit antiserum raised against the α -chain of mucrocetin significantly cross-interacted with the β -chain of mucrocetin (lane 6), indicating the similar antigenicity between these two subunits of mucrocetin.

Platelet-agglutination studies

Mucrocetin strongly induces platelet agglutination in either human PRP or washed platelet suspensions (Figure 2). It appears that mucrocetin agglutinates platelets in a von Willebrand factor (vWf)-independent manner, causing no obvious change of platelet shape. Similar agglutinating activities of mucrocetin in both PRP and washed platelets, with the maximum agglutination achieved at a concentration of about 2.5 $\mu\text{g/ml}$ (18.5 nM), were observed (compare Figure 2A with 2F), suggesting that mucrocetin does not modulate vWf as ristocetin and botrocetin do [3,4]. Moreover, mucrocetin pretreatment had no effect on the aggregation of platelets induced by ristocetin (1.4 mg/ml) in human PRP (Figure 2B and 2C). Purified FL-A at 20 $\mu\text{g/ml}$, which is much higher than the reported IC_{50} [21], completely abolished the aggregation induced by ristocetin in human PRP (Figure 2D), but it did not inhibit the mucrocetin-induced agglutinations in both PRP and washed platelets (Figure 2E and 2H). In addition, a monoclonal antibody CD42b Ab-1, raised against the platelet GPIb, dose-dependently blocked the agglutination induced by mucrocetin with an IC_{50} of 18.1 $\mu\text{g/ml}$ (Figure 2G).

N-terminal partial sequences of mucrocetin

Purified mucrocetins were reduced and S-pyridylethylated, and the dissociated subunits were separated using a reverse-phase HPLC column as described in Materials and Methods. The N-terminal 20 and 26 amino-acid sequences of the two S-pyridylethylated subunits of mucrocetin were determined by Edman degradation. The larger subunit, designated as α , has 25 of its N-terminal 26 residues identical to the α -chain of FL-A [14], while the smaller one, designated as β , is the same as the β -chain of FL-A in their N-terminal 20 residues. In addition, the N-terminal sequences of mucrocetin α and β subunits are also identical to those of TMVA [25], a platelet-aggregating factor isolated from the venoms of geographically remote *Trimeresurus mucrosquamatus* (Chinese habu).

cDNA cloning of mucrocetin

The cDNA encoding for the mucrocetin α -subunit has a nucleotide sequence of 531 bp, which contains the 5'-untranslated primer region of 24 bp, an open reading frame of 474 bp, a stop codon, and the 3'-primer-containing region of 30 bp (The GenBank accession number is AY390533). In addition, the cDNA for the nucleotide sequence of β -subunit is 507 bp, containing the 5'-primer region of 24 bp, an open reading frame of 444 bp, a stop codon, and the 3'-primer-containing region of 36 bp (The GenBank accession number is AY390534). The deduced amino-acid sequences of the α - and β -subunits of mucrocetin revealed a signal peptide of 23 amino-acid residues, followed by mature subunits of 135 and 125 residues, respectively. The predicted N-terminal sequences of α - and β -subunits of mucrocetin are consistent with those by Edman degradation. The calculated molecular masses of α - and β -subunits of mucrocetin are 15,729 Da and 14,542 Da, respectively.

Sequence comparisons

Comparison of the deduced sequences of mature α and β subunits of mucrocetin showed a homology of 39.2%, while the signal peptides of these two subunits are highly similar to each other (95.7% identity). The sequence of α - and β -subunits of mucrocetin have 130 out of 135 and 116 out of 125 amino-acid residues identical to those of FL-A, respectively (Figure 3). Overall, other GPIb-targeting venom proteins were found to share 46.9 ~ 63.5% sequence identity. The α - and β -subunits of mucrocetin bear higher structural similarity (60.7% and 71.2%) to the β - and γ -chains of alboaggregin A, respectively.

Crystal structure determination

In the refined model, deviations from ideal values of bond lengths and angles are within acceptable range. Most amino-acid residues (97.3%) have their (ϕ , ψ) angles in the allowed regions in the Ramachandran plot [26]. Asp ^{α 12} (Asp¹² in α -subunit) and Asp ^{β 12}, with (ϕ , ψ) of about (60, -110), occur in a special glycine-like type II' β -turn [27]. Another glycine-like conformation occurs at Ala ^{α 88}, with (ϕ , ψ) of (85, -30), probably caused by two hydrogen bonds. The disulfide bonds between the cysteine residues α 4– α 15, α 32– α 129, α 81– β 77, α 104– β 121, β 4– β 15, β 32– β 121 and β 98– β 113, as well as the inter-dimer link of α 135– β 3, have good geometry, with bond distances of 2.04 ± 0.01 Å between the sulfur atoms. The final statistics are listed in Table 2. The use of NCS restraints resulted in a root-mean-square deviation (r.m.s.d.) in coordinates of 0.113 – 0.259 Å for 1042 backbone atoms and 1.025 – 1.123 Å for 1085 side-chain atoms between the three heterodimers in an asymmetric unit.

Crystal packing

In the I422 crystal of mucrocetin, the tetramers are organized into 6-layered stacks (or rods) about the crystallographic dyad axis, and these rods are arranged in a mosaic pattern. The 6 tetramers in a rod can be grouped into 3 pairs. The tetramers are related by crystallographic dyad symmetry in the central pair, and by non-crystallographic dyad axes in the top and bottom pairs. The total surface area of each mucrocetin tetramer is about 48000 \AA^2 , while the interface between the tetramers within a pair buries about 3200 \AA^2 areas (80 residues) on each tetramer. In addition, there are two types of contacts between the six-layered rod-like stacks of tetrameric molecules in the mucrocetin crystal. The first type occurs between the molecules related by unit-cell translations in the a-b plane. In other words, each stack is in “lateral” contacts with 4 neighbors. The second type occurs between the molecules related by the body-centering translation. Each stack is in “top-bottom” contacts with 8 neighbors. All of the inter-tetramer contacts comprise hydrogen bonds and salt bridges with no obvious hydrophobic interactions.

The overall structure of mucrocetin and the comparison with flavocetin-A

The overall structure of mucrocetin, made up of four $\alpha\beta$ -heterodimers, is arranged in a square-shaped ring (Figure 4A). This tetrameric ring is stabilized by four inter-dimer “head-to-tail” disulfide linkages of Cys ^{α 135}-Cys ^{β 3} between neighboring heterodimers. The ring has a dimension of approximately $122 \times 122 \times 36 \text{ \AA}^3$, delimiting a large central pore of approximately $65 \times 65 \times 36 \text{ \AA}^3$. Both the two ($\alpha\beta$) subunits in each heterodimer comprise a globular body and an extending loop. The body is composed of five major β -strands and two α -helices and the loop contributes to dimerization with another subunit. An inter-domain disulfide bond between Cys ^{α 81} and Cys ^{β 77} links the swapped loops within each dimer.

The swapped loops are associated with the counter-subunit through an

extensive contact interface, which buries 1770 Å² and 1890 Å² of the 8400 Å² and 8100 Å² total surface areas of α- and β-subunits and involves 36 and 35 amino-acid residues, respectively. Besides the disulfide bond (Cys^{α81}-Cys^{β77}), there are at least 25 direct hydrogen bonds and 12 van der Waals contacts between the two subunits. Interestingly, the segments of residues α71-α75 and β78-β82 formed an inter-molecular anti-parallel beta-like structure. Presumably, this structure and a number of other backbone hydrogen bonds formed in the loop region should contribute to stability of the heterodimer. In contrast, interactions between neighboring heterodimers in the tetrameric mucrocetin are fewer. The interface buries only 400 Å² surface areas and involves 8 residues on each heterodimer. In addition to the disulfide bond (Cys^{α135}-Cys^{β3}), only 5 hydrogen bonds but no VDW interactions were observed.

As shown in Figure 3, the amino-acid sequences of mucrocetin and FL-A have the same lengths of 135 and 125 for α- and β-subunits, respectively, and they differ only in 5 and 9 residues. The three cyclic tetramers in the crystal structure of mucrocetin can be superimposed on the tetramer of FL-A, with r.m.s.d. of 1.149 – 1.266 Å for 1040 pairs of Cα atoms. If the heterodimers are superimposed individually, the r.m.s.d. are 0.709 – 0.824 Å for 260 pairs of Cα atoms. The results appear to be not very different in all three cases. Mucrocetin does not contain bound calcium ion, while the two positively-charged lysine residues Lys^{α130} and Lys^{β122} substituting for the cations in the binding sites, as in FL-A [14], are conserved. The surface potential diagrams of mucrocetin and FL-A show that the former seems to have more negative charges on the molecule, but the theoretical net charges of the two molecules differ by only one unit at neutral pH.

Ten of the fourteen different residues compared with FL-A in mucrocetin are located on the surface of the molecule (see Figure 4B). Except that three residues are

far away from others, Tyr^{α97}, Arg^{α123}, Val^{β54}, Ser^{β58}, His^{β63}, Gln^{β95} and Arg^{β117} are in the vicinity of the concave binding surface and the positions of their side chains are close (Figure 4C). No obvious conformational changes are observed around the regions with residue substitutions. The concave surfaces of mucrocetin molecule are facing outside and are not hindered from binding to effector molecules. Surface-charge comparison of the corresponding region in mucrocetin and FL-A shows significant difference of charge distribution (Figure 4D). In contrast to the structure of FL-A, the side chains of Lys residues at α102, α108, α109, β22, β102 and β116 in mucrocetin tend to point to solvents (Figure 4C). Combined with Arg^{α123} and Arg^{β117}, they form a unique positively-charged patch on the binding surface of mucrocetin (Figure 4D).

DISCUSSION

Binding of plasma vWf to platelet membrane GP Ib-IX-V complex, with exposure to pathologic shear stress (*e.g.*, stenosed arteries), is an important event in triggering thrombosis in embolic stroke and cardiovascular disease [28]. This binding process can be modified by several exogenous modulators, including the C-type lectin-like venom proteins. To date, a number of GPIb-BPs have been isolated from the venoms of crotalid and viperid snakes (Table 1). These venom factors served as useful tools in probing the mechanism of platelet activation and developing a new class of anti-thrombotic agents.

In this paper, we present a GPIb-BP, mucrocetin, isolated from the venom of Taiwan habu (*Trimeresurus mucrosquamatus*). Mucrocetin has a structural organization almost identical to those of FL-A and convulxin [14,29]. The molecular weight of mucrocetin calculated from its amino-acid sequence is 121.1 kDa, smaller than those observed on SDS-PAGE (~135 kDa) and gel-permeation chromatography

(150-200 kDa), indicating a low compactness in mucrocetin molecules. This is in agreement with the crystal structure of mucrocetin, *i.e.*, a square flat ring with a large central pore. Mucrocetin eluted from the anion-exchanger column in the last fractions during the initial isolation step may reflect its acidic property. It is consistent with the observed negative charges on the surface of mucrocetin molecules.

The predicted amino-acid sequence of mucrocetin was confirmed by protein N-terminal sequencing, and the complete sequence is also consistent with its crystal structure, including the distinct residues between mucrocetin and FL-A and those on the concave binding surface. Sequence alignment and comparison of mucrocetin subunits with those of other snake venom GPIb-BPs show various degrees of identity from 38.5% to 60.7% in α -subunit and 52.0% to 71.2% in β -subunit with 24 and 30 identical residues, respectively, suggesting that the β -subunits are more conserved among these lectin-like venom proteins. Kawasaki *et al.* proposed that the GPIb-binding site of venom GPIb-BPs resides on the β -subunit but not the α -subunit [11]. As shown in the structures of mucrocetin and FL-A, the additional Cys¹³⁵ and Cys³ in the α - and β -subunit, respectively, form an inter-dimer “head-to-tail” disulfide linkage. Thus, according to the sequence alignment [30], agglucetin probably possesses a similar interdimer disulfide bridge as well. Nevertheless, these two Cys residues are not found in the sequence of alboaggregin A [15], in spite of its oligomeric feature.

Mucrocetin dose-dependently induced platelet agglutinations on both PRP and washed platelets with similar turbidmetric profiles, indicating that vWf is not needed on the action of mucrocetin, distinguishable from what was observed on botrocetin and bitiscetin [4,5]. The inhibition studies, using FL-A and an anti-GPIb mAb on mucrocetin-induced platelet agglutination, suggest that mucrocetin is a GPIb agonist with a distinct binding site from that of FL-A on GPIb α . In addition, pretreatment of

PRP with mucrocetin showed no effect on the platelet aggregation when stimulated with ristocetin; whereas, agglucetin, in a similar experiment performed by Wang and Huang [16], appeared to markedly prevent such a ristocetin-induced aggregation.

The crystal structure of mucrocetin shows a unique crystal packing of six-layer cylinders of doughnut-shaped molecules. The overall structure of mucrocetin is almost identical to the structures of FL-A and convulxin [14,29], with the $\alpha\beta$ -heterodimer exhibiting the typical backbone fold of carbohydrate-recognition domain (CRD) of C-type lectins [31]. The swapped loops in the $\alpha\beta$ -heterodimer, which are well conserved among the venom GPIb-BPs, are associated with the globular body of the adjacent subunit. The resulting contact interface, corresponding to the C-interface defined in 3D domain swapping [32], buries ~22.4% of the total surface area of one $\alpha\beta$ -heterodimer, thus crucial in connecting the two subunits of mucrocetin. The interface between the $\alpha\beta$ -heterodimers is mainly stabilized by interchain disulfide bridges, only with a few non-covalent interactions.

The distinct behaviors of lectin-like venom proteins to recognize different target molecules, such as coagulation factors, vWf and platelet GPIb, are thought to be in part due to the large hingelike motions at the bases of each swapped loop [19]. Only small movements occur when the venom proteins target on similar molecules. Consistently, the backbone chain of mucrocetin superimposes well with that of FL-A, and the relative orientations of the α - and β -subunits of these two proteins are almost identical. The structure of bitiscetin-vWf A1 complex reported by Maita *et al.* suggested that a positively-charged patch on the α -subunit of bitiscetin may interact with the C-terminal anionic region of GPIb α [33]. However, this basic patch of bitiscetin was not observed in the structures of mucrocetin and flavocetin-A. In addition, two hydrophilic patches were observed in the structure of FL-A β -subunit [14], which are considered as possible candidates for the platelet GPIb-binding sites.

In the structure of mucrocetin, these two peptide fragments were shown to exist as well (Figure 3). The central part of the concave surface in mucrocetin appears to bear more concentrated positive charges than that of FL-A (Figure 4D), though the overall negative charges of mucrocetin structure are slightly greater. Thus, based on these observations, the disparate platelet effects between mucrocetin and FL-A are likely the consequence of different charge distributions on the putative binding surface. Namely, the unique positively-charged patch formed by several Lys and Arg residues on mucrocetin appears to be the primary determinant of the platelet-agglutinating activity of mucrocetin.

The crystal structures of platelet GPIb α and its complexes with vWf A1 domain or thrombin have been published [34-36]. Three negatively-charged patches on the surface of GPIb α were localized to regions that interact with vWf A1 domain and the exosites I and II of thrombin, respectively. The interacting surfaces between GPIb α and its bound ligands show the heterogeneous charge distributions and reflect striking charge complementarities. These acidic patches on GPIb α may be the candidates of mucrocetin-targeting site. More structural studies of mucrocetin in complex with GPIb α are needed to elucidate the proposed interaction mechanism.

ACKNOWLEDGEMENTS

This work was supported by grants from Academia Sinica (A. H.-J. Wang) and National Science Council (S.-H. Chiou). We are grateful to Dr. Jeu-Ming P. Yuann and Dr. Yuh-Ling Chen of the Institute of Biological Chemistry at Academia Sinica (Taipei, Taiwan) for kindly providing fresh whole blood and helpful discussion on platelet-agglutination assay, respectively. We thank Dr. Yuch-Cheng Jean of the National Synchrotron Radiation Research Center (Hsinchu, Taiwan) for assistance in X-ray data collection.

REFERENCES

- 1 Roth, G. J. (1991) Developing relationships: arterial platelet adhesion, glycoprotein Ib, and leucine-rich glycoproteins. *Blood* **77**, 5-19
- 2 Ruggeri, Z. M. (1999) Structure and function of von Willebrand factor. *Thromb. Haemost.* **82**, 576-584
- 3 Azuma, H., Sugimoto, M., Ruggeri, Z. M. and Ware, J. (1993) A role for von Willebrand factor proline residues 702-704 in ristocetin-mediated binding to platelet glycoprotein Ib. *Thromb. Haemost.* **69**, 192-196
- 4 Fukuda, K., Doggett, T. A., Bankston, L. A., Cruz, M. A., Diacovo, T. G. and Liddington, R. C. (2002) Structural basis of von Willebrand factor activation by the snake toxin botrocetin. *Structure* **10**, 943-950
- 5 Matsui, T., Hamako, J., Matsushita, T., Nakayama, T., Fujimura, Y. and Titani, K. (2002) Binding site on human von Willebrand factor of bitiscetin, a snake venom-derived platelet aggregation inducer. *Biochemistry* **41**, 7939-7946
- 6 Fujimura, Y., Kawasaki, T. and Titani, K. (1996) Snake venom proteins modulating the interaction between von Willebrand factor and platelet glycoprotein Ib. *Thromb. Haemost.* **76**, 633-639
- 7 Andrews, R. K. and Berndt, M. C. (2000) Snake venom modulators of platelet adhesion receptors and their ligands. *Toxicon* **38**, 775-791
- 8 Polgar, J., Magnenat, E. M., Peitsch, M. C., Wells, T. N., Saqi, M. S. and Clemetson, K. J. (1997) Amino acid sequence of the α subunit and computer modelling of the α and β subunits of echicetin from the venom of *Echis carinatus* (saw-scaled viper). *Biochem. J.* **323**, 533-537
- 9 Chen, Y. L., Tsai, K. W., Chang, T., Hong, T. M. and Tsai, I. H. (2000) Glycoprotein Ib-binding protein from the venom of *Deinagkistrodon acutus*--cDNA sequence, functional characterization, and three-dimensional

- modeling. *Thromb. Haemost.* **83**, 119-126
- 10 Andrews, R. K., Kroll, M. H., Ward, C. M., Rose, J. W., Scarborough, R. M., Smith, A. I., Lopez, J. A. and Berndt, M. C. (1996) Binding of a novel 50-kilodalton alboaggregin from *Trimeresurus albolabris* and related viper venom proteins to the platelet membrane glycoprotein Ib-IX-V complex. Effect on platelet aggregation and glycoprotein Ib-mediated platelet activation. *Biochemistry* **35**, 12629-12639
- 11 Kawasaki, T., Fujimura, Y., Usami, Y., Suzuki, M., Miura, S., Sakurai, Y., Makita, K., Taniuchi, Y., Hirano, K. and Titani, K. (1996) Complete amino acid sequence and identification of the platelet glycoprotein Ib-binding site of *jararaca* GPIb-BP, a snake venom protein isolated from *Bothrops jararaca*. *J. Biol. Chem.* **271**, 10635-10639
- 12 Sakurai, Y., Fujimura, Y., Kokubo, T., Imamura, K., Kawasaki, T., Handa, M., Suzuki, M., Matsui, T., Titani, K. and Yoshioka, A. (1998) The cDNA cloning and molecular characterization of a snake venom platelet glycoprotein Ib-binding protein, mamushigin, from *Agkistrodon halys blomhoffii* venom. *Thromb. Haemost.* **79**, 1199-1207
- 13 Shin, Y., Okuyama, I., Hasegawa, J. and Morita, T. (2000) Molecular cloning of glycoprotein Ib-binding protein, flavocetin-A, which inhibits platelet aggregation. *Thromb. Res.* **99**, 239-247
- 14 Fukuda, K., Mizuno, H., Atoda, H. and Morita, T. (2000) Crystal structure of flavocetin-A, a platelet glycoprotein Ib-binding protein, reveals a novel cyclic tetramer of C-type lectin-like heterodimers. *Biochemistry* **39**, 1915-1923
- 15 Kowalska, M. A., Tan, L., Holt, J. C., Peng, M., Karczewski, J., Calvete, J. J. and Niewiarowski, S. (1998) Alboaggregins A and B. Structure and interaction with human platelets. *Thromb. Haemost.* **79**, 609-613

- 16 Wang, W. J. and Huang, T. F. (2001) A novel tetrameric venom protein, agglucetin from *Agkistrodon acutus*, acts as a glycoprotein Ib agonist. *Thromb. Haemost.* **86**, 1077-1086
- 17 Mizuno, H., Fujimoto, Z., Koizumi, M., Kano, H., Atoda, H. and Morita, T. (1997) Structure of coagulation factors IX/X-binding protein, a heterodimer of C-type lectin domains. *Nature Struct. Biol.* **4**, 438-441
- 18 Mizuno, H., Fujimoto, Z., Atoda, H. and Morita, T. (2001) Crystal structure of an anticoagulant protein in complex with the Gla domain of factor X. *Proc. Natl. Acad. Sci. U.S.A.* **98**, 7230-7234
- 19 Hirotsu, S., Mizuno, H., Fukuda, K., Qi, M. C., Matsui, T., Hamako, J., Morita, T. and Titani, K. (2001) Crystal structure of bitiscetin, a von Willebrand factor-dependent platelet aggregation inducer. *Biochemistry* **40**, 13592-13597
- 20 Huang, K. F., Hung, C. C., Wu, S. H. and Chiou, S. H. (1998) Characterization of three endogenous peptide inhibitors for multiple metalloproteinases with fibrinogenolytic activity from the venom of Taiwan habu (*Trimeresurus mucrosquamatus*). *Biochem. Biophys. Res. Commun.* **248**, 562-568
- 21 Taniuchi, Y., Kawasaki, T., Fujimura, Y., Suzuki, M., Titani, K., Sakai, Y., Kaku, S., Hisamichi, N., Satoh, N., Takenaka, T., Handa, M. and Sawai, Y. (1995) Flavocetin-A and -B, two high molecular mass glycoprotein Ib binding proteins with high affinity purified from *Trimeresurus flavoviridis* venom, inhibit platelet aggregation at high shear stress. *Biochim. Biophys. Acta* **1244**, 331-338
- 22 Mustard, J. F., Perry, D. W., Ardlie, N. G. and Packham, M. A. (1972) Preparation of suspensions of washed platelets from humans. *Br. J. Haematol.* **22**, 193-204
- 23 Otwinowski, Z. and Minor, W. (1997) Processing of X-ray diffraction data collected in oscillation mode. *Methods Enzymol.* **276**, 307-326
- 24 Brunger, A. T., Adams, P. D., Clore, G. M., Delano, W. L., Gros, P.,

- Grosse-Kunstleve, R. W., Jiang, J. S., Kuszewski, J., Nilges, M., Pannu, N. S., Read, R. J., Rice, L. M., Simonson, T. and Warren, G. L. (1998) Crystallography & NMR system: a new software suite for macromolecular structure determination. *Acta Crystallog. sect. D* **54**, 905-921
- 25 Wei, Q., Lu, Q. M., Jin, Y., Li, R., Wei, J. F., Wang, W. Y. and Xiong, Y. L. (2002) Purification and cloning of a novel C-type lectin-like protein with platelet aggregation activity from *Trimeresurus mucrosquamatus* venom. *Toxicon* **40**, 1331-1338
- 26 Laskowski, R. A., MacArthur, M. W., Moss, D. S. and Thornton, J. M. (1993) PROCHECK: a program to check the stereochemical quality of protein structures. *J. Appl. Cryst.* **26**, 283-291
- 27 Richardson, J. S. (1981) The anatomy and taxonomy of protein structure. *Adv. Protein Chem.* **34**, 167-339
- 28 Ruggeri, Z. M. (2002) Platelets in atherothrombosis. *Nature Med.* **8**, 1227-1234
- 29 Murakami, M. T., Zela, S. P., Gava, L. M., Michelin-Duarte, S., Cintra, A. C. O. and Arni, R. K. (2003) Crystal structure of the platelet activator convulxin, a disulfide-linked $\alpha_4\beta_4$ cyclic tetramer from the venom of *Crotalus durissus terrificus*. *Biochem. Biophys. Res. Commun.* **310**, 478-482
- 30 Wang, W. J., Ling, Q. D., Liau, M. Y. and Huang, T. F. (2003) A tetrameric glycoprotein Ib-binding protein, agglucetin, from Formosan pit viper: structure and interaction with human platelets. *Thromb Haemost.* **90**, 465-75
- 31 Weis, W. I., Kahn, R., Fourme, R., Drickamer, K. and Hendrickson, W. A. (1991) Structure of the calcium-dependent lectin domain from a rat mannose-binding protein determined by MAD phasing. *Science* **254**, 1608-1615
- 32 Bennett, M. J., Schlunegger, M. P. and Eisenberg, D. (1995) 3D domain swapping: a mechanism for oligomer assembly. *Protein Sci.* **4**, 2455-2468

- 33 Maita, N., Nishio, K., Nishimoto, E., Matsui, T., Shikamoto, Y., Morita, T., Sadler, J. E and Mizuno, H. (2003) Crystal structure of von Willebrand factor A1 domain complexed with snake venom, bitiscetin: insight into glycoprotein Ib α binding mechanism induced by snake venom proteins. *J. Biol Chem.* **278**, 37777-37781
- 34 Huizinga, E. G., Tsuji, S., Romijn, R. A., Schiphorst, M. E., de Groot, P. G., Sixma, J. J. and Gros, P. (2002) Structures of glycoprotein Ib α and its complex with von Willebrand factor A1 domain. *Science* **297**, 1176-1179
- 35 Dumas, J. J., Kumar, R., Seehra, J., Somers, W. S. and Mosyak, L. (2003) Crystal structure of the GpIb α -thrombin complex essential for platelet aggregation. *Science* **301**, 222-226
- 36 Celikel, R., McClintock, R. A., Roberts, J. R., Mendolicchio, G. L., Ware, J., Varughese, K. I. and Ruggeri, Z. M. (2003) Modulation of α -thrombin function by distinct interactions with platelet glycoprotein Ib α . *Science* **301**, 218-221

FIGURE LEGENDS

Figure 1 Isolation of mucroctin from *Trimeresurus mucrosquamatus* venom

Crude *Trimeresurus mucrosquamatus* venom was separated on a TSK DEAE-650 anion-exchanger column by a two-step linear gradient of ammonium bicarbonate. The eluates that contain mucroctins (indicated with an arrow) were then subjected to purification by the successive gel-filtration chromatographies as described in Materials and Methods. Purified proteins were checked on SDS-PAGE (lanes 1-4, *inset*), or blotted to PVDF membrane for immunological analysis using an antiserum raised against the α -subunit of mucroctin (lanes 5-8, *inset*). Lanes 2, 4 6 and 8 were loaded with mucroctin, and lanes 1,3 5 and 7 were samples of purified flavocetin-A. M: the pre-stained protein markers with molecular masses as indicated. R: reduced. NR: non-reduced.

Figure 2 Platelet-agglutination studies

Platelet-agglutination assays were carried out in either human platelet-rich plasma (PRP) (A-E) or washed platelet suspensions (F-H). (A) Platelet agglutination was initiated by the addition of various concentrations of mucroctin as indicated. (B) Platelet aggregation was triggered by the addition of the platelet inducer ristocetin. (C) Ristocetin was added 3 min after addition of mucroctin. (D) and (E) Platelets were preincubated with flavocetin-A for 3 min, and then ristocetin and mucroctin were added, respectively. (F) Typical patterns of platelet agglutination caused by various concentrations of mucroctin in washed platelet suspensions. (G) Washed platelets were preincubated with various concentrations of the anti-GPIb mAb CD42b Ab-1, as indicated, for 3 min, and subsequently mucroctin was added to trigger platelet agglutination. (H) Three min after addition of flavocetin-A, mucroctin was added to washed platelet suspension. All of these agglutination responses were continuously monitored by turbidmetry and expressed as an increase in light transmission. One of

duplicate experiments is presented here.

Figure 3 Sequence comparison of mucrocetin with flavocetin-A

Identical residues in flavocetin-A are denoted with “-“. The two hydrophilic patches previously observed in the structure of flavocetin-A [14], which are proposed to involve in GPIIb-binding, are shaded.

Figure 4 Overall structure of mucrocetin and the concave binding surface on the molecule

(A) Four heterodimers of the mucrocetin α (red) and β (green) subunits are arranged about a four-fold axis as shown with a ribbon diagram. Within a dimer (lower panel), the two subunits are associated by swapping of the loop-domains and a inter-subunit disulfide bridge, shown as ball-and-stick models. There are three other disulfide bonds within each subunit. The heterodimers are further connected by intermolecular, head-to-tail, disulfide bonds to form a circular tetramer. (B) The space-filling model of mucrocetin molecule denotes the substituted residues (magenta) on the surface of mucrocetin as compared with those in flavocetin-A. The mucrocetin α - and β -subunits are painted in yellow and cyan, respectively. (C) The $2F_o - F_c$ maps (contoured at the 1.0σ level) of mucrocetin around some residues located at the concave binding surface are presented. The density maps for the substituted residues are drawn in cyan and those for the Lys residues that contribute to the positive charges of the binding surface are shown in yellow. (D) Diagrams of the surface charge potential on the mucrocetin (upper) and flavocetin-A (lower) molecules are shown. The surfaces are drawn in red, white and blue for negative, neutral and positive charges, respectively. The views are facing the concave binding surface on these two molecules.

Table 1 Comparison of various platelet GPIb α -targeting venom proteins

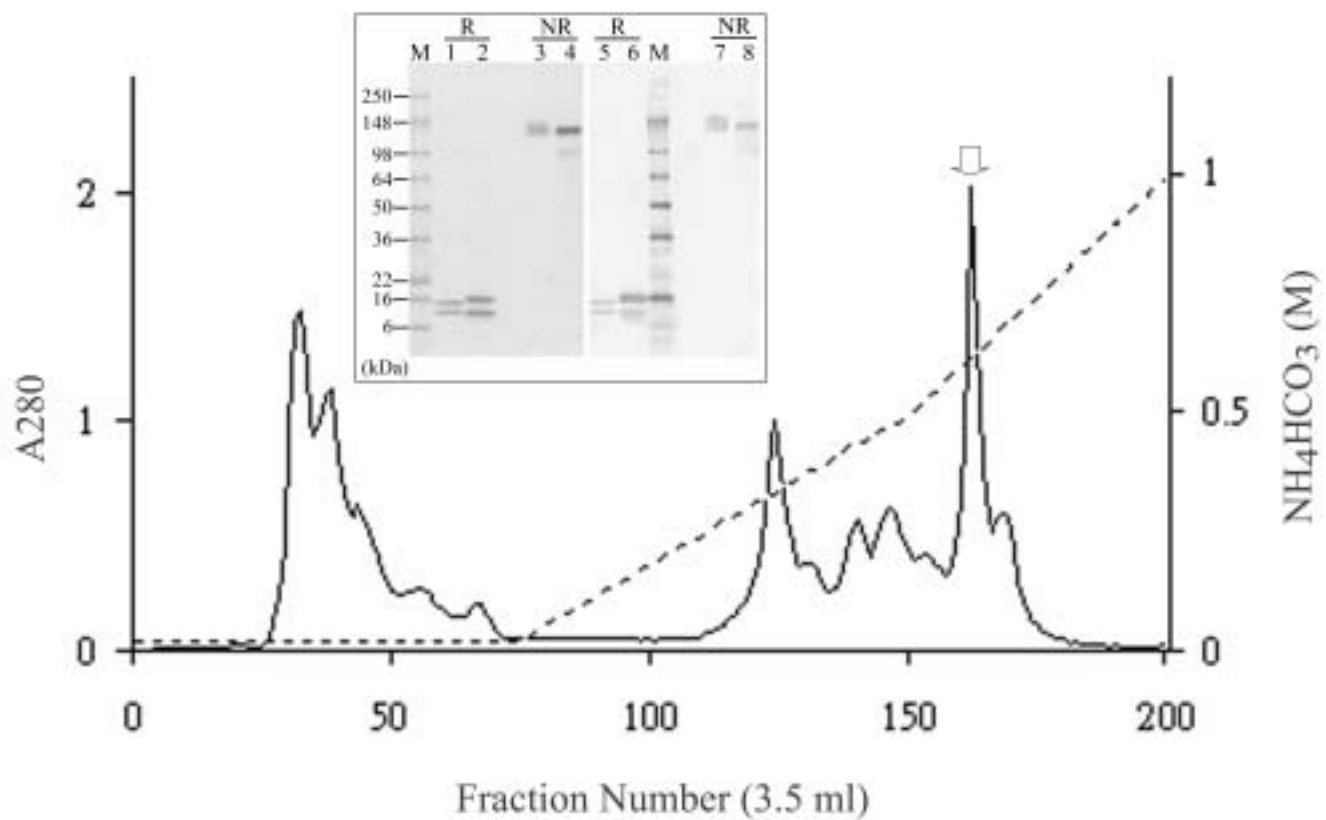
	Subunit structure	Extra disulfide bridges for oligomerization	Action	MAbs with similar or adjacent binding sites on GPIb α
Flavocetin A (<i>Trimeresurus flavoviridis</i>)[14]	($\alpha\beta$) ₄	yes	antagonist	GUR83-35 [†]
Echicetin (<i>Echis carinatus</i>)[8]	$\alpha\beta$	no	antagonist	AK2 and SZ2
Agkicetin-C (<i>Agkistrodon acutus</i>)[9]	$\alpha\beta$	no	antagonist	AK2
Jararaca GPIb-BP (<i>Bothrops jararaca</i>)[11]	$\alpha\beta$	no	antagonist	AP1
Mamushigin (<i>Agkistrodon halys blomhoffi</i>)[12]	$\alpha\beta$	no	antagonist	AP1
CHH-B (<i>Crotalus horridus horridus</i>)[10]	$\alpha\beta$	no	antagonist	AK2
Alboaggregin A (<i>Trimeresurus albolabris</i>)[15]	$\alpha\beta\delta\gamma$	yes	agonist	AK2 and SZ2 (adjacent) [‡]
Alboaggregin B (<i>Trimeresurus albolabris</i>)[15]	$\alpha\beta$	no	agonist	AK2 and SZ2
Agglucetin (<i>Agkistrodon acutus</i>)[16]	$\alpha_1\alpha_2\beta_1\beta_2$	yes	agonist	AP1 and LJ-Ib1
Mucrocetin (<i>Trimeresurus mucrosquamatus</i>)	($\alpha\beta$) ₄	yes	agonist	CD42b Ab-1 [§]

[†]Targeting sites of these mAbs on platelet GPIb are as follows: GUR83-35 and LJ-Ib1, within His1-Arg293 of GPIb α ; AK2, Leu36-Gln59; SZ2, Tyr276-Glu282; AP1, Phe201-Gly268. [‡]Alboaggregin A, performed in a cross-blocking study [10], strongly blocked AK2 and only partially blocked SZ2 binding to GPIb α . [§]A mAb was produced by using both GPIb α - and β -chain as antigen.

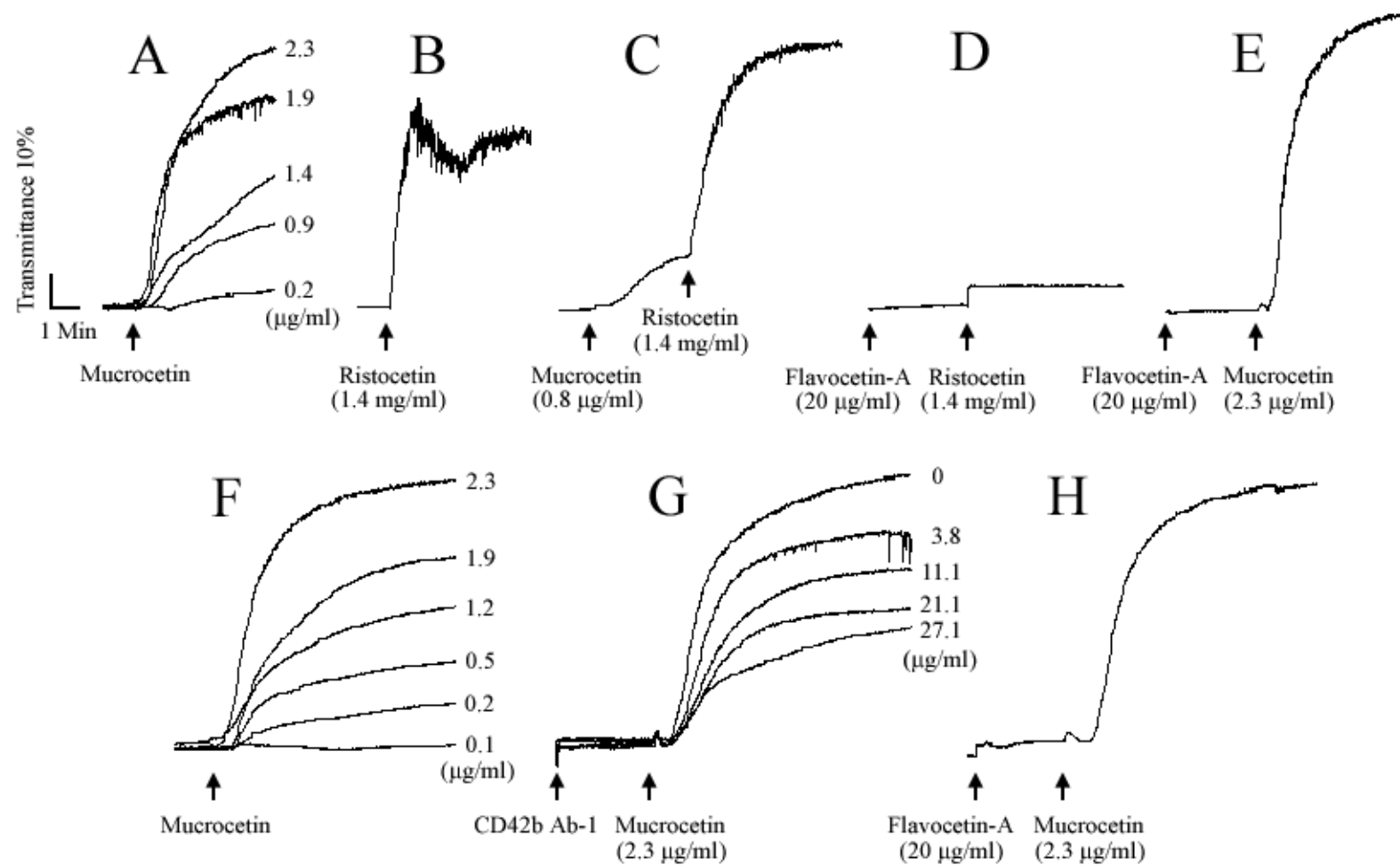
Table 2 Crystallographic statistics of mucrocetin

Data collection		
Space group	I422	
Unit cell dimension (Å)	$a = b = 119.9, c = 360.8$	
Resolution range (Å)	20 – 2.8	(2.9 – 2.8) [§]
Number of observations	127,650	(12,356)
Unique reflections	30,509	(2,971)
Completeness (%)	92.9	(92.3)
Average $I/\sigma(I)$	11.5	(2.9)
R_{merge} (%)	10.0	(48.2)
Refinement		
Resolution range (Å)	18 – 2.8	
R-factor for 95% working data set [$>0 \sigma(F)$]	0.235	
R_{free} for 5% test data set	0.294	
r.m.s.d. from ideal bond lengths (Å)	0.012	
r.m.s.d. from ideal bond angles (°)	1.68	
Ramachandran plot: Number of non-proline and non-glycine residues		
in most favored regions (%)	77.3	
in additional allowed regions (%)	20.0	
Average B-value for 6381 protein atoms (Å ²)	52.2	
for 601 water molecules (Å ²)	47.9	

[§]Numbers in parentheses are for the highest resolution shells.



-----Fig.1. Huang *et al.*-----



-----Fig. 2. Huang *et al.*-----

α subunit

```

1         10         20         30         40         50
|         |         |         |         |         |
mucroetin  $\alpha$   DFDCIPGWSAYDRYCYQAFSEPKNWEDAESFCEEGVKTSHLVSI ESSGEG
flavocetin-A  $\alpha$  -----K-----

        60         70         80         90         100
        |         |         |         |         |
mucroetin  $\alpha$   DFVAQLVAEKIKTSFQYVWIGLRIQNKEQQCRSEWSDASSVNYENLYKQS
flavocetin-A  $\alpha$  -----V--F

        110        120        130   135
        |         |         |         |
mucroetin  $\alpha$   SKKCYALKKGT ELRTWFNVYCGRENPFVCKYTPEC
flavocetin-A  $\alpha$  -----T--E-----
    
```

β subunit

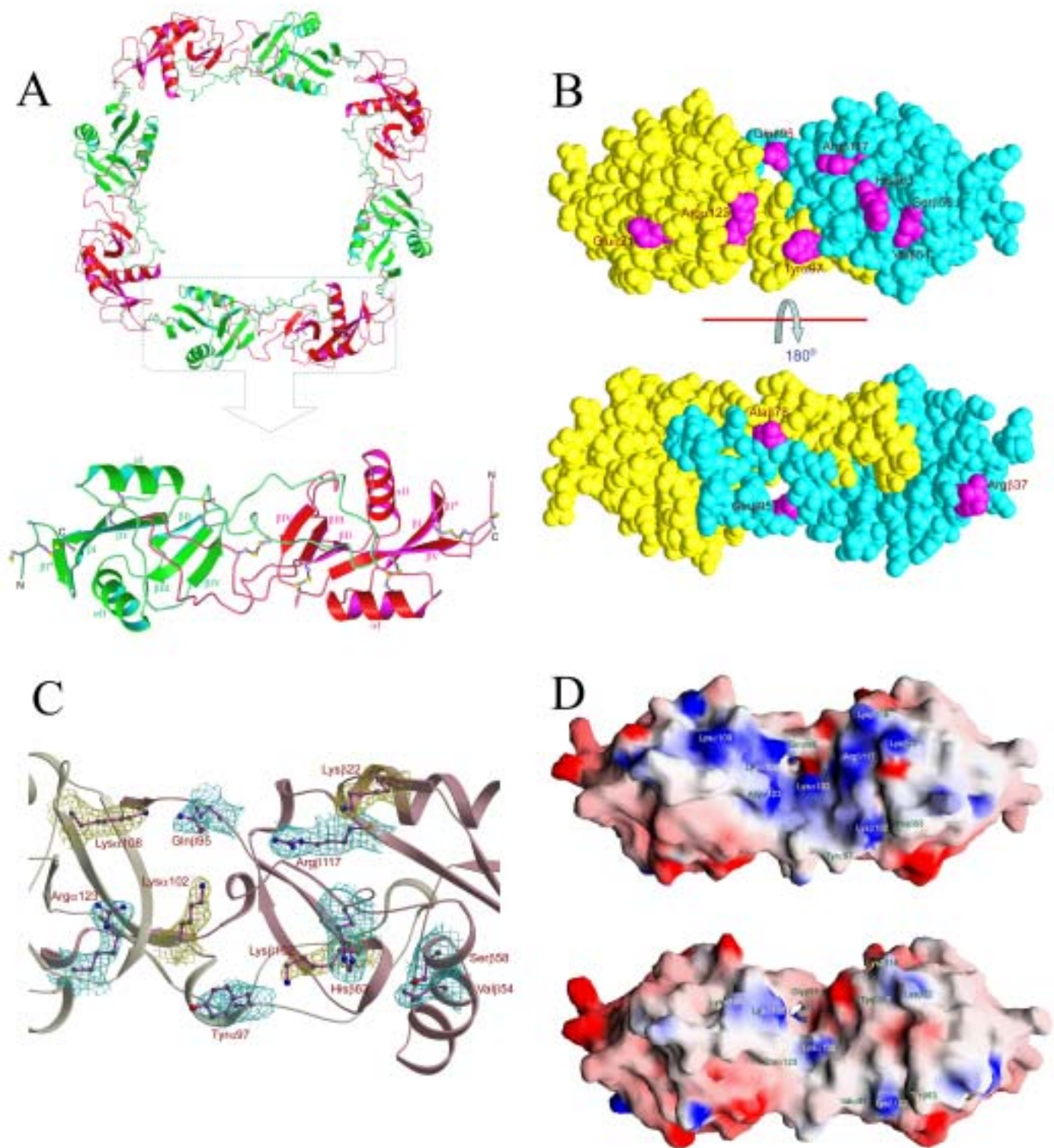
```

1         10         20         30         40         50
|         |         |         |         |         |
mucroetin  $\beta$   GFCCPLGWSSYDEHCYQVFQQKMNWEDA EK FCTQQHRGSHLVSFH SSEEV
flavocetin-A  $\beta$  -----K-----

        60         70         80         90         100
        |         |         |         |         |
mucroetin  $\beta$   DFVVSKTSPILKHDFVWMGLSNVWNECAKEWSDGTKLDYKAWSGQSDCIT
flavocetin-A  $\beta$  ---T--F---Y---I-----T-----G---V

        110        120   125
        |         |         |
mucroetin  $\beta$   SKTTDNQWLSMDCSSKRYVVCKFQA
flavocetin-A  $\beta$  -----Y-----
    
```

-----Fig. 3. Huang *et. al.*-----



-----Fig. 4. Huang *et al.*-----